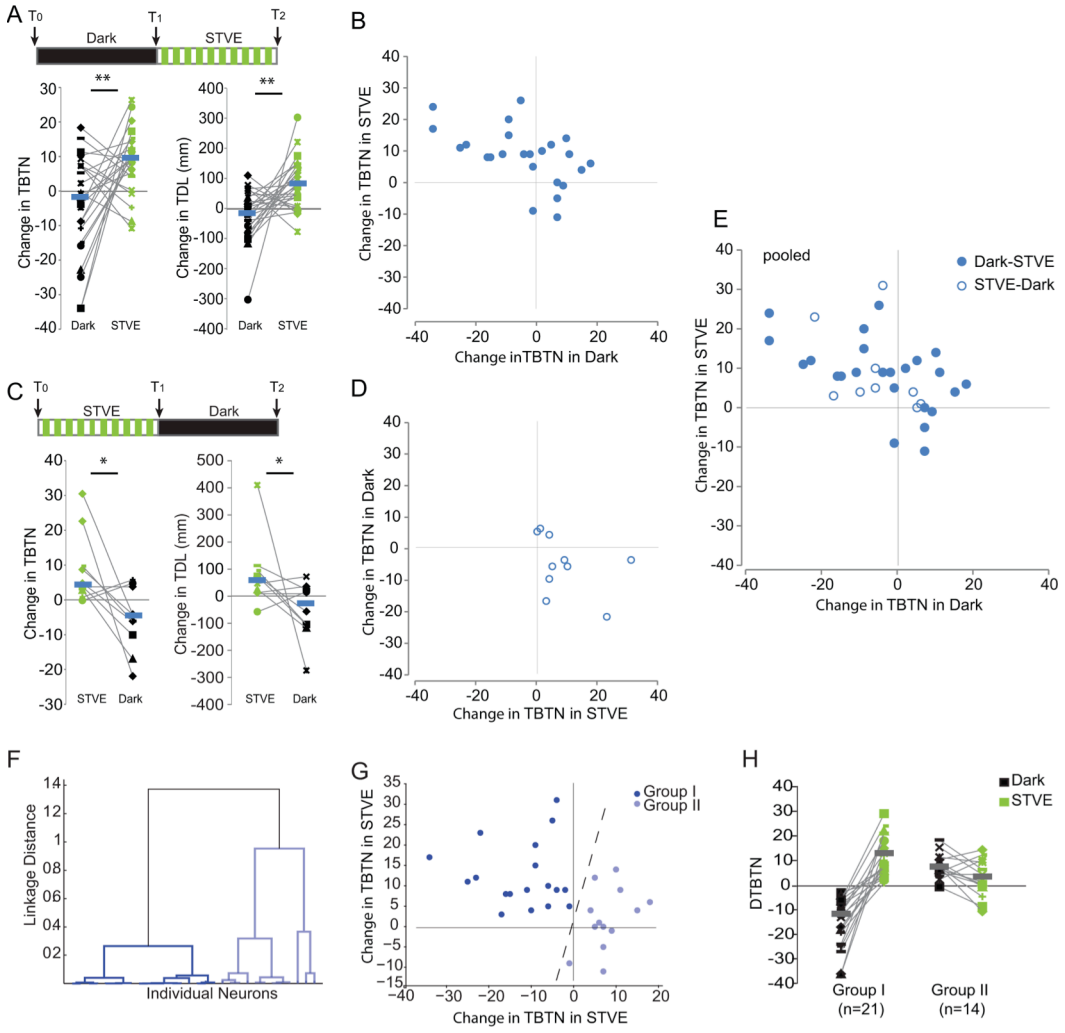

Figure S1, related to Figures 2 and 3. STVE promotes dendritic arbor growth in excitatory tectal neurons. A. Change in total branch tip number (TBTN) and total dendritic length (TDBL) in response to dark and short term visual enhancement (STVE) in excitatory neurons (n=25). Medians are marked by blue bars. Inset: schematic of experimental paradigm, animals were subjected to 4 hours of dark followed by 4 hours of STVE. Arrows show the imaging time points. B. Scatter plots of changes in TBTN of individual neurons in response to dark vs. STVE. C. Average change in TBTN and TDBL of excitatory neurons in response to STVE and dark (n=10). Inset shows schematic of experimental paradigm. Animals were subjected to 4 hours of STVE followed by 4 hours of dark. D. Scatterplots of changes in TBTN of individual neurons in response to STVE vs. dark E. Scatter plot of the data pooled from both dark-STVE and STVE-dark paradigms of excitatory neurons. Error bars in all figures are S.E.M. *: $p<0.05$, *: $p<0.01$, Wilcoxon sign rank test. F-H. Cluster analysis of excitatory neurons. F. Dendrogram of unsupervised hierarchical clustering analysis of excitatory neuronal population based on changes in TBTN in response to dark and STVE. G. Scatterplot of individual data showing the clustered result. D. Summarized change in TBTN of the two groups in response to dark and STVE. Numbers in parentheses show the number of neurons in each group. Gray bars mark the mean value of each group. One group shows bimodal plasticity with dark/STVE where TBTN decreases with dark and increases with STVE. The other group shows modest increases in TBTN in dark and STVE.

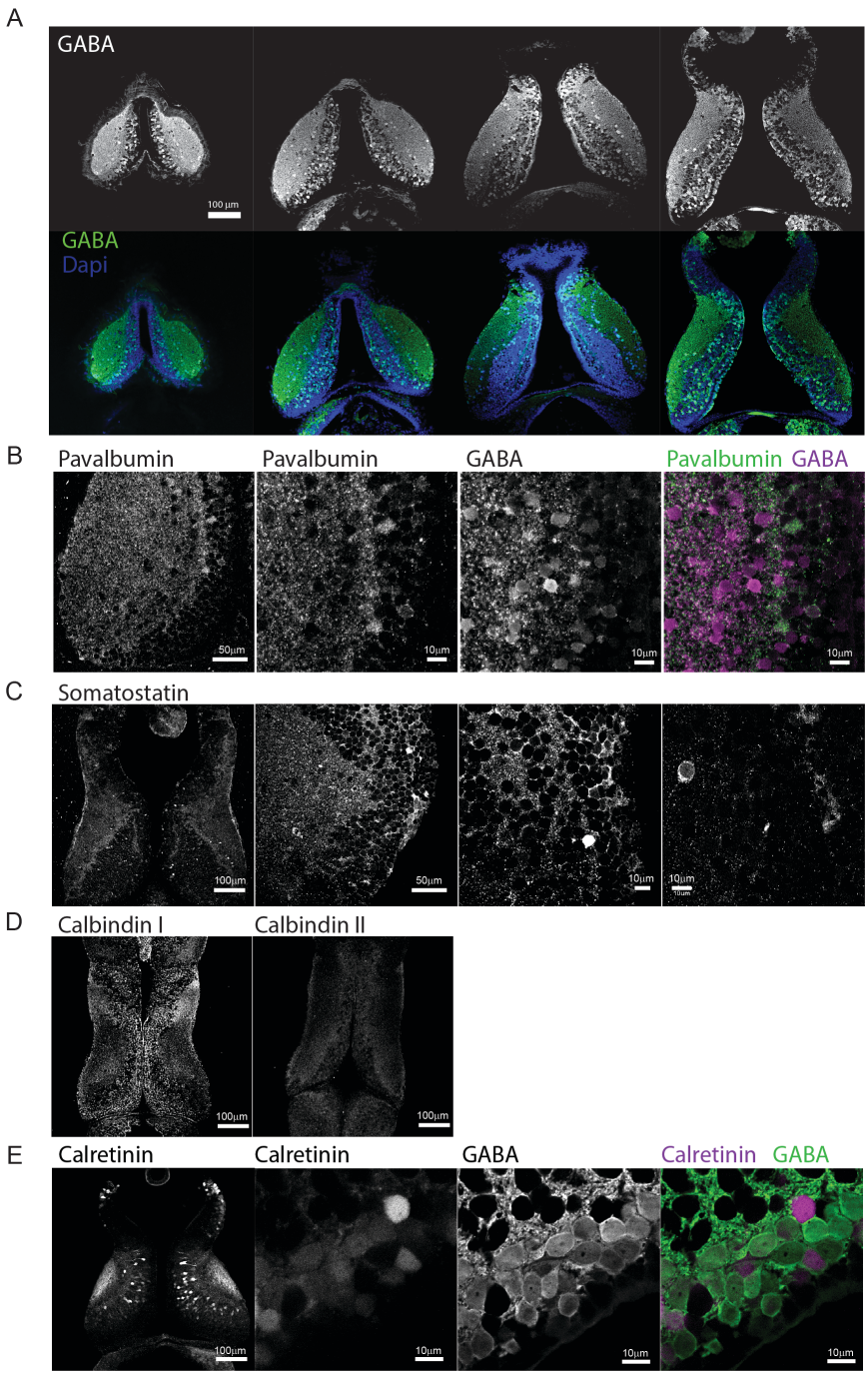

Figure S2, related to Figure 3. Immunostaining for GABA and different GABA-related Ca binding proteins in the optic tectum of st 47-48 tadpoles. A. GABA staining with Dapi signals shows the distribution of inhibitory neurons in the tectum, optic sections left to right are from dorsal to ventral. B. Pavalbumin signal was detectable but PV+ soma was only sporadic. PV+ soma is also GABA+. C. somatostatin expression level is also very low at this stage in the tectum, with only sporadic SOM+ cell soma. D. No reliable calbindin I or II signal could be detected in the tectum at this stage. E. Calretinin immunostaining shows strong signal in the tectum, but some CRT+ soma are GABA-, suggesting not all CRT+ neurons are inhibitory at this stage.

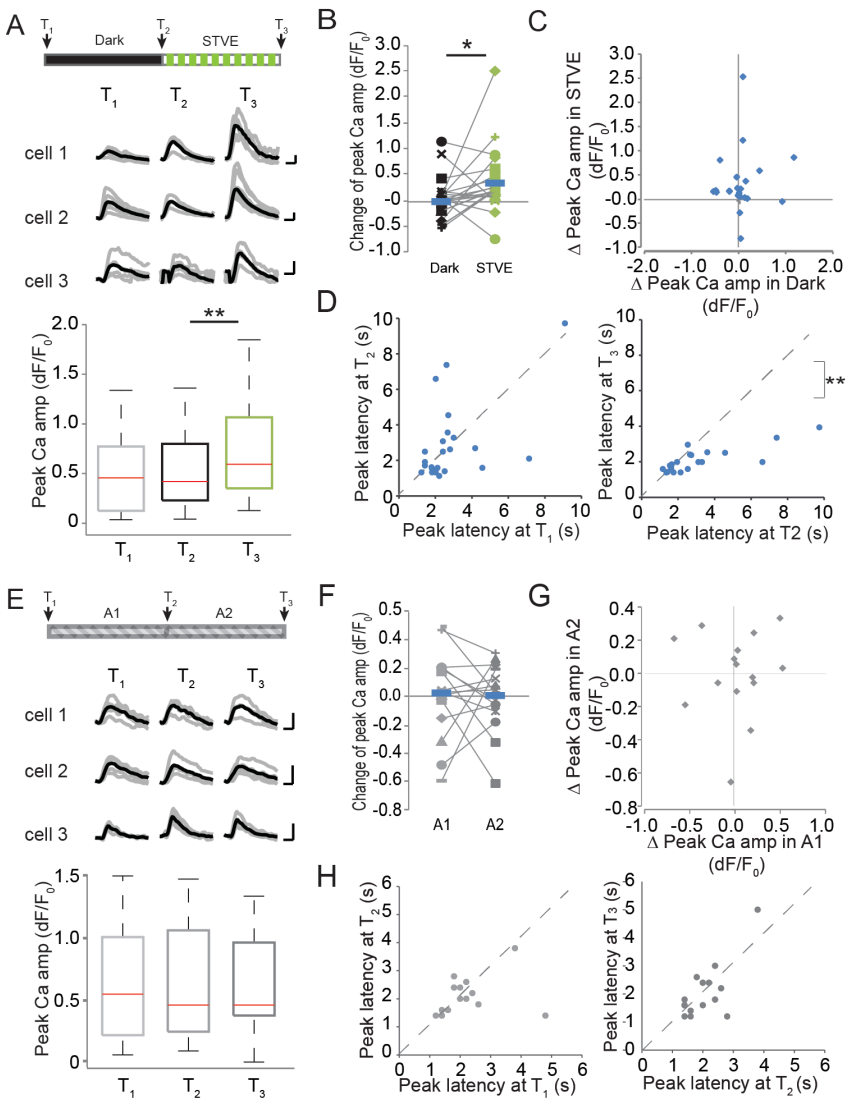

Figure S3, related to Figure 5. STVE but not ambient light increases visually-evoked Ca responses in excitatory neurons. A. Top: Representative visually-evoked Ca traces of individual excitatory neurons at each time point. Gray: single trials; Dark: averaged traces. Scale bar: 2 sec, 100% dF/F_0. Bottom: Average peak response at each time point (n=22). **: $p<0.01$, Wilcoxon sign rank test. B. Changes in the Ca peak amplitude during dark and STVE. Blue bars mark the medians. *: $p<0.05$, Wilcoxon sign rank test. C. Scatter plots of changes in Ca response for individual excitatory neurons (STVE vs. Dark). D. Scatter plots of peak latency of Ca response in E and I neurons at T_2 vs. T_2 and T_3 vs. T_3. **: $p<0.01$, Wilcoxon sign rank test. E. Top: Representative visual-evoked Ca traces of individual excitatory neurons in animals subjected to two consecutive ambient light sessions (A1-A2). Bottom: Average Ca peak amplitude at different time points in the A-A paradigm. F. Changes in the Ca response amplitude during the two ambient sessions in excitatory neurons (n=15). G. Scatter plots of changes in Ca response for individual excitatory neurons (A2 vs. A1). H. Scatter plots of peak latency of Ca response in at T_2 vs. T_1 and T_3 vs. T_2.

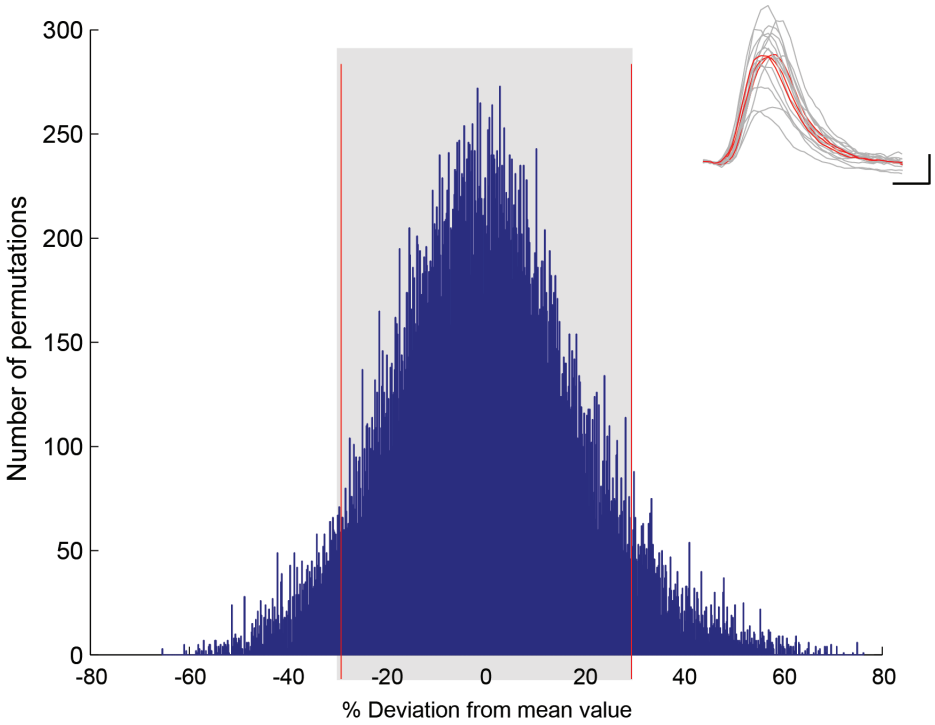

Figure S4, related to Figure 5 and Experimental Procedures. Histogram of distribution of 10000 permutations of repeated measurements of visually evoked calcium responses from single neurons. 15 ~20 measurements of each neuron were randomly permutated to calculated the average response of every 5 measurements. The number of permutations were plotted against the deviation from the total mean value of each neuron (total n=7). The shaded area marks the 95% confidence range. Inset: example of Ca traces from one single neuron. Gray: raw responses from single trials; Red: average responses of 3 5-trial sets. Scale bar: 100% dF/F_0, 2sec.

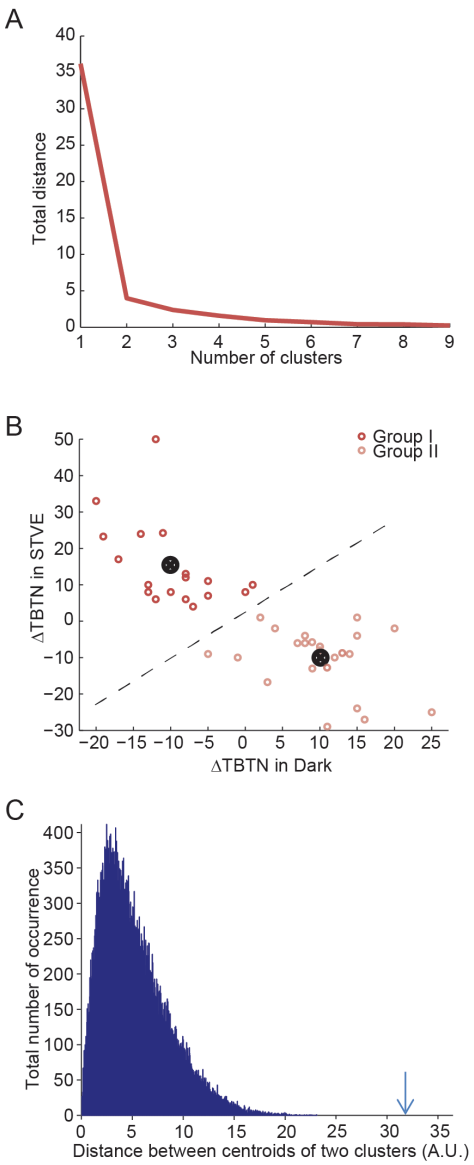

Figure S5, related to Experimental Procedures. Cluster analysis with k-mean method. A. Elbow test based on changes in TBTN showing that the sharpest drop of the total distance occurs when cluster number equals 2, which is conventionally selected as the number of clusters for k-means approach considering the bias-variance tradeoff. B. Clustering results with k-mean clustering analysis based on ΔTBTN. The dark solid circles show the centroids for each cluster. Note that this clustering result is consistent with the clustering result using the hierarchical clustering analysis. C. Distribution of the Euclidean distance between the centroids of two randomly assigned clusters with 100000 permutations. Arrow shows the actual distance between centroids of the two clusters identified by the unsupervised hierarchical method ($p < 0.00001$).

Table S1, related to Experimental Procedures. Cophenetic correlation coefficient of different metrics for hierarchical cluster analysis

metric	Cophenetic correlation coefficient
Euclidean	0.770066
sEuclidean	0.758741
cityblock	0.767575
minKowski	0.770066
mahalanobis	0.79203
cosine	**0.960311**
hamming	0.910924
jaccard	0.910924

Table notes: multiple metrics that applicable to the dataset were tested and the one gives the highest Cophenetic correlation coefficient (in bold) was chosen for the final analysis.

Supplemental Experimental Procedures

Animal Care

Albino Xenopus laevis embryos were obtained from either in-house mating or from Xen Express (Brooksville, FL), and reared at 22-23°C with 12 hrs dark/12 hrs light cycle in 0.1X Steinberg's solution (58.0 mM NaCl, 0.67 mM KCl, 0.34 mM $Ca(NO_3)_2$, 0.83 mM $MgSO_4$, 3.0 mM HEPES, pH 7.2). Animals were fed from stage 47 and were housed individually in 6-well plates from the first day of imaging. All animal protocols were approved by the Institutional Animal Care and Use Committee of the Scripps Research Institute.

Tectal Cell Transfection

Animals were electroporated with specified DNA constructs at the stage of 45-46 (Nieuwkoop and Faber, 1956) and were screened for sparsely transfected tectal cells a week after electroporation at st47-48. The detailed protocol of electroporation has been described previously (Bestman and Cline, 2008; Bestman et al., 2012). In short, tadpoles were anesthetized in 0.01% MS222 (3- aminobenzoic acid ethyl ester, Sigma-Aldrich) and DNA plasmids (1-3μg/μl, in ddH2O and mixed with fast-green) were injected into the midbrain ventricle. Platinum electrodes were positioned on each side of the tadpole brain centering on the tectum. Electrical current was delivered through a Grass SD9 stimulator (34V, 1.6 msec duration), 1-2 pulses were applied with each polarity.

DNA Constructs

For single cell time lapse structural imaging experiments, the Gal4-UAS binary system was used to ensure high expression for GFP. Gal4 was expressed under the control of rat VGAT promoter (gift from Dr. B. Condie) (Oh et al., 2005). Although the VGAT promoter does not drive expression exclusively in GABAergic neurons by electroporation, it does increase the probability of expression in GABAergic neurons in the tectum (unpublished observation). The VGAT-Gal4 construct was co-electroporated with a UAS-e1b-eGFP construct, which has a minimal e1b promoter under 14 repeats of the gal4 response element UAS. For functional imaging of visually-evoked Ca response, pGP-CMV-GCaMP6s was a gift from Douglas Kim (Addgene plasmid # 40753).

In Vivo Time Lapse Imaging of Dendritic Structure and Data Analysis

Animals were electroporated with DNA constructs at stage of 45-46 and screened for those with sparsely transfected and well-isolated cells and were pre-screened under epifluorescent microscope to select those with very sparsely transfected and well-isolated cells, usually with one or two neurons in the whole tectum. For imaging, animals were anesthetized with 0.01% MS-222 (Sigma) and were placed in a Sylgard chamber covered by glass coverslip. Images were collected at the same time daily, or every 4hr for the visual experience manipulation experiments. Two-photon z-series were collected at 1 μm steps with a 20x water immersion objective (Olympus XLUMPlanFL 0.95NA) at 3-4x scan zoom using a custom built microscope modified from an Olympus FV300 system, which had been described in details in (Bestman and Cline, 2008; Ruthazer et al., 2006).

The raw image stacks were imported into Imaris (Bitplane, US). Complete dendritic arbors of each neuron were reconstructed using a semi-manual function in the Filament module of Imaris. Total dendritic length and branch tip number were automatically calculated by the software. 3D Sholl analysis calculates the number of branches that intersect with concentric circles at increasing distances from the cell soma and was done using a customized Matlab program with reconstructed filament data exported from Imaris. Branch dynamic analysis was accomplished using a customized C++ software 4DSPA (Lee et al., 2013).

In Vivo Time Lapse Imaging of Visually Evoked Calcium Responses and Data Analysis

For functional imaging based on Calcium responses, animals were pre-screened for those with sparsely transfected neurons electroporated with GCaMP6s-expressing constructs (Chen et al., 2013). On the day of imaging, animals were immobilized with pancuronium dibromide (1μM in 0.1X Steinberg solution; Tocris, Ellisville, MO) for 5 minutes (Dunfield and Haas, 2009). The animal was then placed in a customized cylinder shaped acrylic clear chamber (6.8 cm diameter, 6 cm height) filled with freshly aerated Steinberg's solution for Calcium imaging. The side wall of the chamber was covered with back projecting screen material (Screen Solutions International, Rocklin, CA) to display the visual stimulus. Visual stimuli were generated with CogGphTB tool box in Matlab and were presented through a pocket projector (Optoma, Shenzhen, China) using a video converter (AGPtek High Resolution Video VGA Conversion VGA to RCA Composie/S-Video Converter Box). Visual stimuli were full screen light on stimuli (1 second duration, with 10 seconds inter-stimulus interval, and 5 repeats) and were passed through a red

filter (HQ607/45M, Chroma) to prevent interference with the GCaMP signal. The shape of the stimuli was pre-warped to correct for the arc shape of the chamber wall. During imaging, the animal was covered with 1% low-melting agarose (Lonza #50101, Rockland, ME) in 0.1X Steinberg's solution for extra immobilization. The same two-photon microscope and objective described above were used for calcium imaging. The optic tectum was imaged with a zoom factor of 2. To achieve a 5 Hz scanning rate, single optical section of a clip with the size of 512x72 pixels (355x50 μm^2 area) encompassing the neuron of interest was imaged. A wavelength of 940 nm was used to excite GCaMP6s. The visual stimulus was simultaneously recorded in the red channel.

Time-series of calcium response data were processed in Image J (NIH) by manually identifying the region of interest (cell soma) and then further analyzed with customized Matlab scripts. Visually evoked increases in GCaMP6 fluorescence was calculated as dF/F_0, where F_0 was the average intensity over 1 second immediately preceding the onset of the stimulus and dF is the difference between F_0 and the fluorescence intensity at any given time point. The temporal correlation between the calcium signals and the visual stimuli were calculated. Cells with responses that were not temporally correlated to stimuli were not included in further analysis. Tectal neurons at this stage are known to show response to light-ON, light-Off or both type of stimuli, with the majority showing strong responses to light-off stimulus. Due to the slow dynamics of Ca++ responses and the 1 second stimulus on duration, we cannot reliably distinguish ON-response from Off-response, so the quantification likely reflects a combination of both, presumably mostly Off response. To determine the variability (replicability) of individual neuronal responses to visual stimuli at any given time point, we recorded responses to 15-20 repeats of visual stimuli in a subset of neurons. We then used bootstrap to calculate the 95% confidence range of variation with any 5 repetitions was [-29%, 31%] of the mean value (Figure S4), which means any change in the peak amplitude that is beyond this range of the initial response amplitude could be considered significantly different from the initial response. By this criteria, for the dark-STEV data set, 46/49 inhibitory neurons and 20/22 excitatory neurons showed significant change in Ca amplitude during at least one of the visual manipulation sessions. For the Ambient-Ambient data set, 11/16 inhibitory neurons and 12/15 excitatory neurons showed significant change in Ca amplitude during at least one of the sessions.

Immunohistochemistry and Post Hoc Identification of GABAergic Neurons

Immediately after the last time point of imaging, animals were fixed with freshly made 4% PFA and 2% Glutaraldehyde (Electron Microscopy Sciences, Fort Washington, PA) in 1xPBS (pH 7.4) using a Pelco BioWave Pro microwave (Model 36500, Ted Pella, Redding, CA. 350mV on 20 sec, off 20 sec, on 20 sec, followed by 150mV on 1 min, off 1 min, on 1 min). The animals were then transferred to fresh fixative and post-fixed at 4C overnight. The next day, the animals were washed in 1xPBS using the microwave (150mV on-off-on, 1min each). The brain was then dissected and washed in 1XPBS for up to an hour at room temperature and then embedded in 20% chicken albumin (with 0.15% gelatin) cross linked by 1% glutaraldehyde. 30mm vibratome sections were cut for free floating immunofluorescence staining. Sections were incubated in 1% Sodium Borohydride (Sigma) in 1xPBS for 15 min to quench auto fluorescence, blocked in 10% normal goat serum (Jackson Lab, ME) in PBS with 2% Triton X-100 (PBST) for one hour in room temperature, followed by incubation in rabbit anti GABA polyclonal antibody (Sigma A2052, RRID: AB_477652, 1:2000 in PBST with 1% normal goat serum) for 48 hours at 4 C. Secondary antibody (goat anti rabbit Alexa Fluor 633, Thermo Fisher Scientific Cat# A-21070, RRID: AB_2535731) was diluted 1:500 in PBST and incubated for an hour at room temperature. After 3 15min rinses with PBS, sections were mounted on slides in Vectashield Mounting Medium with Dapi (Vector Laboratories, Burlingame, CA). For immuno-staining without GABA antibody, animals were fixed in 4% PFA. Primary antibodies used include mouse anti parvalbumin antibody (Millipore Cat# MAB1572, RRID: AB_2174013), rabbit anti somatostatin antibody (Novus Cat# NB110-61682, RRID: AB_965461), rabbit anti calbindin I and calbindin II antibodies (Aviva Systems Biology Cat# ARP60104_P050, RRID: AB_10872740 and Aviva Systems Biology Cat# ARP58600_P050, RRID: AB_2045271), rabbit anti calretinin (Abcam Cat# ab702, RRID: AB_305702).

Images for posthoc immunostained sections were collected either on a Fluoview 500 confocal microscope (Olympus) or a Nikon C2 confocal microscope (Nikon). Both the eGFP and GCaMP6 fluorescence signal was well preserved in the fixed tissue, thus no antibody was needed for visualization. Z-stacks images were taken under low magnification (20x air objective) to find the neuron that had been imaged in vivo. The corresponding neurons were confirmed by their location in the tectum, the dendritic arbor branching patterns as well as (in the case of GCaMP-expressing samples) neighboring transfected cell patterns. High magnification images were then taken at > 3 different z-depth through the soma to examine GABA immunoreactivity in the soma. In details, a large area (usually encompassed both cell body layer and neuropil layer of the tectum) was selected in each immunohistochemistry image. The histogram of the distribution of the intensity of pixels within the selected area was examined and the intensity value

corresponding to the peak count in the histogram (or the first peak, in rarer cases where two peaks were present) was set as the background threshold. Neuronal soma with average pixel intensity above the threshold was deemed as GABA positive. Samples with poor GABA immunostaining were not included in the final data set.

Time-lapse imaging of experience-dependent structural and functional plasticity in the same neuron

To image full dendritic arbor and visually-evoked Ca^{++} responses in the same neuron, we co-electroporated animals at stage 45-46 with pGP-CMV-GCaMP6s (4μg/ul, Addgene plasmid # 40753) and aact-Gal4-UAS-tdTomato (0.8μg/ul). Electrical current was delivered through a Grass SD9 stimulator (34V, 1.6 msec duration), 1-2 pulses were applied with each polarity. The electroporation parameters were tinkered to achieve an expression level of the tdTomato that is bright enough for structural imaging but not too bright that its immature green phase completely masks the GCaMP6 signal within the soma. Animals were pre-screened 7-10 days after electroporation for those with very sparsely transfected and well-isolated cells expressing tdTomato and showing discernable visually-evoked Ca^{++} responses. Animals were subjected to either 4hr dark followed by 4hr STVE or 4hr STVE alone and time-lapse images of both dendritic structure and visually-evoked Ca^{++} responses were collected at time points before and after each visual manipulation session. Two-photon z-series of the complete dendritic arbors were collected at 1 μm steps with a 20x water immersion objective (Olympus XLUMPlanFL 0.95NA) at 3~4x scan zoom using a custom built microscope modified from an Olympus FV300 system (Bestman and Cline, 2008; Ruthazer et al., 2006). Time series of visually-evoked Ca^{++} responses were collected at 30Hz frame rate on a Scientifica multiphoton resonant microscope (Scientifica, UK) with a 25x water immersion objective (Olympus ultra 25xMPE, 1.05NA). Wavelength of 940nm was used for both structural and functional 2P imaging.

In vivo patch clamp recording

Tadpoles at stage 47 were either put into a visual stimulation chamber with LED arrays for 4 hours (short term visual enhancement, STVE), or left on the bench top under ambient light (Control). Whole cell in vivo patch clamp recordings were performed as previously described (Shen et al., 2011). For in vivo recordings, the brains were placed in a custom-made chamber with extracellular saline containing (in mM: 115 NaCl, 2 KCl, 3 $CaCl_2$, 1.5 $MgCl_2$, 5 HEPES, 10 glucose, and 0.01 glycine, pH 7.2, osmolality 255 mOsm). The internal solution contains (in mM) K-Gluconate 95, $MgCl_2$-$6H_2O$ 1.5, Na_2-phosphocreatine 10, KCl 13, HEPES 20, EGTA 10, ATP 4, GTP 0.3, and creatine phosphokinase 10 units/ml. Recording micropipettes were pulled from borosilicate glass capillaries (Warner Instruments, Hamden, CT) with a pipette puller (P-97, Sutter Instrument, Novato, CA) and had resistances in the range of 7–9 MΩ. Excitatory compound synaptic currents (eCSCs) and inhibitory CSCs (iCSCs) were recorded while holding the membrane potential at -60 mV and 0 mV, respectively. Full-field visual stimuli with luminance of 20cd/m^2 were presented from a projector (Samsung SP-P310ME). Each stimulus was presented 10 times at a frequency of 0.1 Hz with an interval of 0.05 Hz (i.e. 10 sec on and 20 sec off). All cells were recorded from the middle portion along the rostrocaudal axis of the tectum. Signals were filtered at 2 kHz with a Multiclamp 700B amplifier (Molecular Devices, Palo Alto, CA) and a Digidata 1440A data acquisition system (Molecular Devices). Data were sampled at 10 kHz with Clampex 10 (Molecular Devices) and analyzed using Clampfit 10 (Molecular Devices) or MATLAB (The MathWorks, Natick, MA). Because the majority of tectal neurons at these stages show predominant light-off responses, we analyzed the excitatory compound synaptic currents (eCSCs), and inhibitory CSCs (iCSCs) to light-off stimuli. Both the fast (within 50msec after the offset of the stimulus) and the total (within 500msec after the offset of the stimulus) integrated response showed similar results and only the total integrated response results were reported.

Cluster analysis and statistics

Custer analysis was performed on the corresponding datasets using an unsupervised agglomerative hierarchical tree method in MATLAB (linkage.m) based upon their pair-wise vectorial distance in the constructed 2D space (pdist.m). The threshold was arbitrarily set at the highest level that can separate the dataset into two clusters. For the choice of metrics used for the cluster analysis, we first compared several metrics that are applicable to our dataset (Table S1) and selected the one that yielded the highest Cophenetic correlation coefficient for the final analysis shown in Figure 3. The cophenetic correlation coefficient is a measurement of the fidelity with which the relationships in the dendrogram represent the raw dataset. In addition, we applied k-means clustering analysis initiated with random seeds and used the elbow test to determine the number of clusters. The total distance versus number of cluster curve suggested that two-cluster approach is the best solution for our dataset (the elbow) considering the bias-variance tradeoff (Figure S5A). For our dataset, k-means clustering also revealed two clusters, which were identical to the clusters identified by the unsupervised hierarchical clustering analysis (Figure S5B). Lastly, by using a bootstrap approach, we randomly permuted the cluster labels and calculated a 'null distribution' for the Euclidean distance

between the centroids of the randomly generated clusters and found that the Euclidean distance between the centroids of the two clusters identified by the hierarchical cluster analysis is significantly larger than the randomly generated distances (number of permutation: 100,000, $p<0.00001$, Figure S5C).

Nonparametric statistical analysis was performed in all statistical tests. Wilcoxon sign rank test was performed for within-cell comparison. Kruskal-Wallis test with posthoc Mann-Whitney U test were performed when comparing data across different groups of neurons under different visual experiences. The statistical test used for each experiment is specified in the results.

Supplemental References:

Bestman, J.E., and Cline, H.T. (2008). The RNA binding protein CPEB regulates dendrite morphogenesis and neuronal circuit assembly in vivo. Proc Natl Acad Sci U S A 105, 20494-20499.
Bestman, J.E., Lee-Osbourne, J., and Cline, H.T. (2012). In vivo time-lapse imaging of cell proliferation and differentiation in the optic tectum of Xenopus laevis tadpoles. The Journal of comparative neurology 520, 401-433.
Chen, T.W., Wardill, T.J., Sun, Y., Pulver, S.R., Renninger, S.L., Baohan, A., Schreiter, E.R., Kerr, R.A., Orger, M.B., Jayaraman, V., et al. (2013). Ultrasensitive fluorescent proteins for imaging neuronal activity. Nature 499, 295-300.
Dunfield, D., and Haas, K. (2009). Metaplasticity governs natural experience-driven plasticity of nascent embryonic brain circuits. Neuron 64, 240-250.
Lee, P.C., He, H.Y., Lin, C.Y., Ching, Y.T., and Cline, H.T. (2013). Computer aided alignment and quantitative 4D structural plasticity analysis of neurons. Neuroinformatics 11, 249-257.
Nieuwkoop, P., and Faber, J. (1956). Normal Table of Xenopus laevis (Daudin). (Amsterdam: Elsevier-North Holland Publishing Co).
Oh, W.J., Noggle, S.A., Maddox, D.M., and Condie, B.G. (2005). The mouse vesicular inhibitory amino acid transporter gene: expression during embryogenesis, analysis of its core promoter in neural stem cells and a reconsideration of its alternate splicing. Gene 351, 39-49.
Ruthazer, E.S., Li, J., and Cline, H.T. (2006). Stabilization of axon branch dynamics by synaptic maturation. J Neurosci 26, 3594-3603.
Shen, W., McKeown, C.R., Demas, J.A., and Cline, H.T. (2011). Inhibition to excitation ratio regulates visual system responses and behavior in vivo. J Neurophysiol 106, 2285-2302.